

Supplement of Atmos. Meas. Tech., 11, 1565–1582, 2018
<https://doi.org/10.5194/amt-11-1565-2018-supplement>
© Author(s) 2018. This work is distributed under
the Creative Commons Attribution 4.0 License.



Supplement of

Bootstrap inversion technique for atmospheric trace gas source detection and quantification using long open-path laser measurements

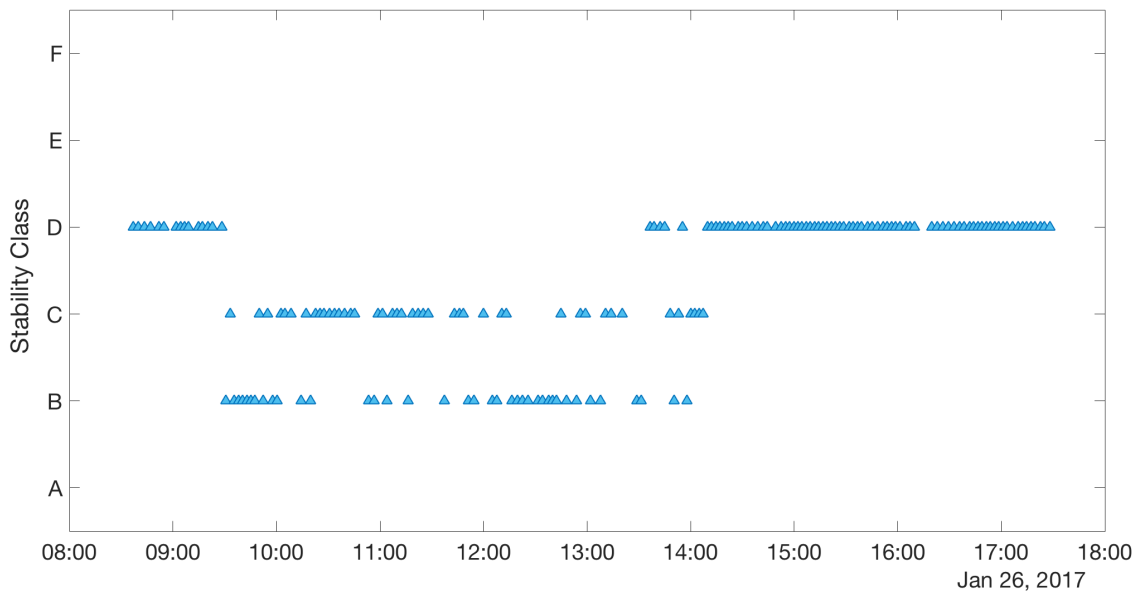
Caroline B. Alden et al.

Correspondence to: Caroline B. Alden (caroline.alden@colorado.edu)

The copyright of individual parts of the supplement might differ from the CC BY 4.0 License.

Pasquill-Gifford Atmospheric Stability Class

Stability classes for each time period of the field data collected on 1/26/2017 are determined following Turner's Method (Turner, 1964), as outlined in section 6.4.1 of the U.S. EPA's Meteorological Monitoring Guidance for Regulatory Modeling Applications Meteorological Monitoring Guidance Table 6-5 (Bailey, 2000). For each measurement time, we follow the procedure outlined in Table 6-6 of that report to determine the Net Radiation Index number. The first step is to calculate solar altitude and use Table 6-5 in that report to determine the insolation class number. The second step is to modify the insolation number based on total cloud cover, which we estimate based on the difference between expected maximum and actual downwelling solar radiation as measured at Table Mountain (our field site) by the National Oceanic and Atmospheric Administration (NOAA) Earth System Research Laboratory (ESRL) Surface Radiation Network (SURFRAD). That data is available at the following FTP site ftp://aftp.cmdl.noaa.gov/data/radiation/surfrad/Boulder_CO/. Further information specific to the SURFRAD site located at our field site on Table Mountain can be accessed here: <https://www.esrl.noaa.gov/gmd/grad/surfrad/tablemt.html>. We do not have information about the ceiling at Table Mountain, so modifications of the insolation class number for ceiling height are not made. The third step is to determine the stability class for each time period using the derived Net Radiation Index number and measured wind speed in Table 6-4.



15

Figure S1: Timeseries of stability class calculated for Table Mountain field site on 01/26/2017.

20

As a sensitivity test, we examine the use of dispersion coefficients that are based on 10-minute empirical data for our 2-minute datasets. We calculate the expected potential error introduced in σ_y using the standard equation for the adjustment of dispersion parameters for different averaging times:

$$\sigma_{y,2} = \sigma_{y,1} \left(\frac{t_2}{t_1} \right)^p, \quad (S1)$$

5 found in Gifford (1976).

The Briggs parameters used in this study were calculated using an averaging time of 10 minutes, so that $t_1 = 10$ minutes (Briggs, 1974; Griffiths, 1994). We use measurements averaged over 2 minutes and meteorological data averaged over 2 minutes, so that $t_2 = 2$ minutes. Using the typical value of 0.2 for the empirical parameter p (for $t_2 < 1$ hour) (Gifford, 1976),
 10 we calculate that a factor of 0.7 correction should be applied to the Briggs horizontal dispersion coefficient, σ_y . We are not aware of similar adjustment formulas for the vertical dispersion coefficient.

We apply the correction factor to the field data collected on January 26th, 2017 (the synthetic data has no time dimension, and transport is considered perfect in that observing system simulation experiment, so the choice of the dispersion coefficient
 15 has less bearing on the findings). The results are seen in Table S1.

	<u>Source Location 1</u>	<u>Source Location 2</u>
Controlled Leak Time On:	10:08	NA
Controlled Leak Time Off:	16:30	NA
Measured Mean Flow Rate:	3.1 E-5 ± 0.01E-5 kg s ⁻¹	0.0 ± 0.0 kg s ⁻¹
Non-Bootstrap Solution:	2.4 E-5 kg s ⁻¹	0.5 E-5 kg s ⁻¹
NZMB Solution:	2.6 E-5 ± 0.5 E-5 k/s	0.0 ± 0.0 kg s ⁻¹

Table S1: Same as Table 2 in the main text, but calculated with an adjustment to the dispersion coefficient, σ_y . Controlled methane release flow rates and 1 standard deviation for each field experiment, including local time that leak was turned on and off.

The recovered fluxes do not change to within a detectable range. It is possible that the sensitivity of our result to the
 20 adjustment to σ_y is low because the cross-wind fluctuations are largely averaged through by the laser beam when winds are orthogonal to the beam. The histograms of the solutions shown in Table S1 are shown below.

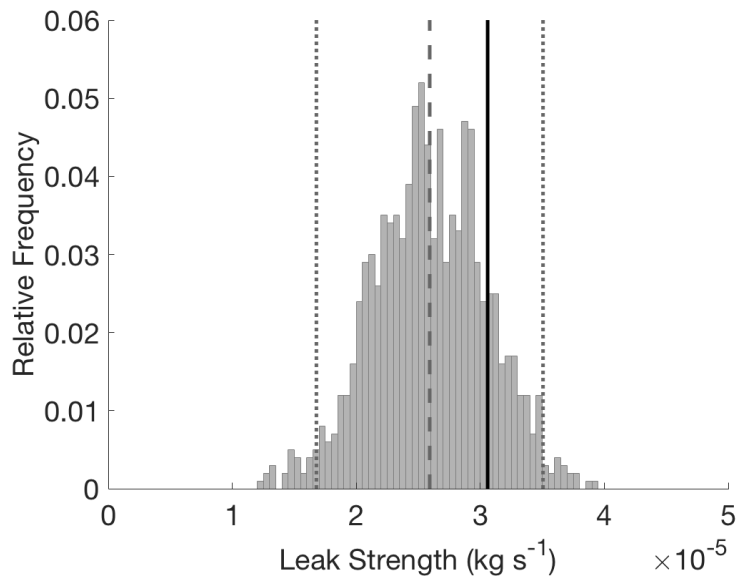


Figure S2: Same as Figure 11 in the main text, but calculated with an adjustment to the dispersion coefficient, σ_y . Histogram of NZMB estimated source strength at source location 1, with dashed line showing the bootstrap mean and thin dotted lines showing ± 2 standard deviation. The thick black line shows the true leak strength at source location 1 ($3.1 \text{ E-5 kg s}^{-1}$).

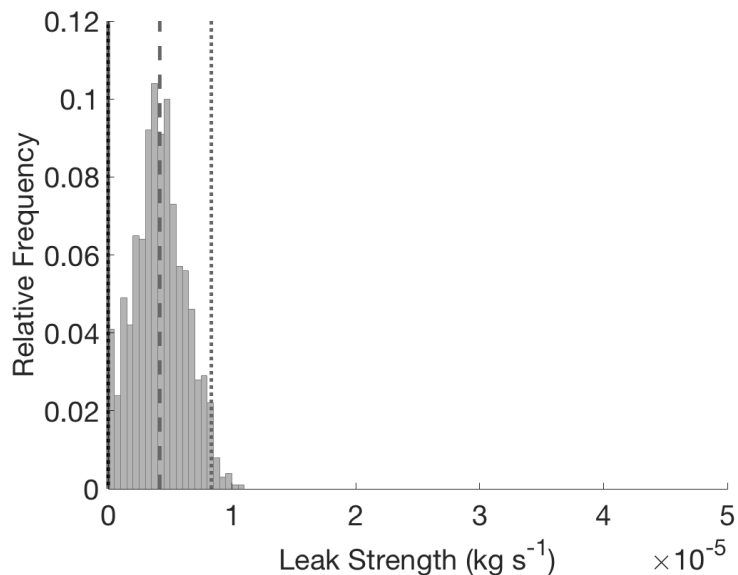


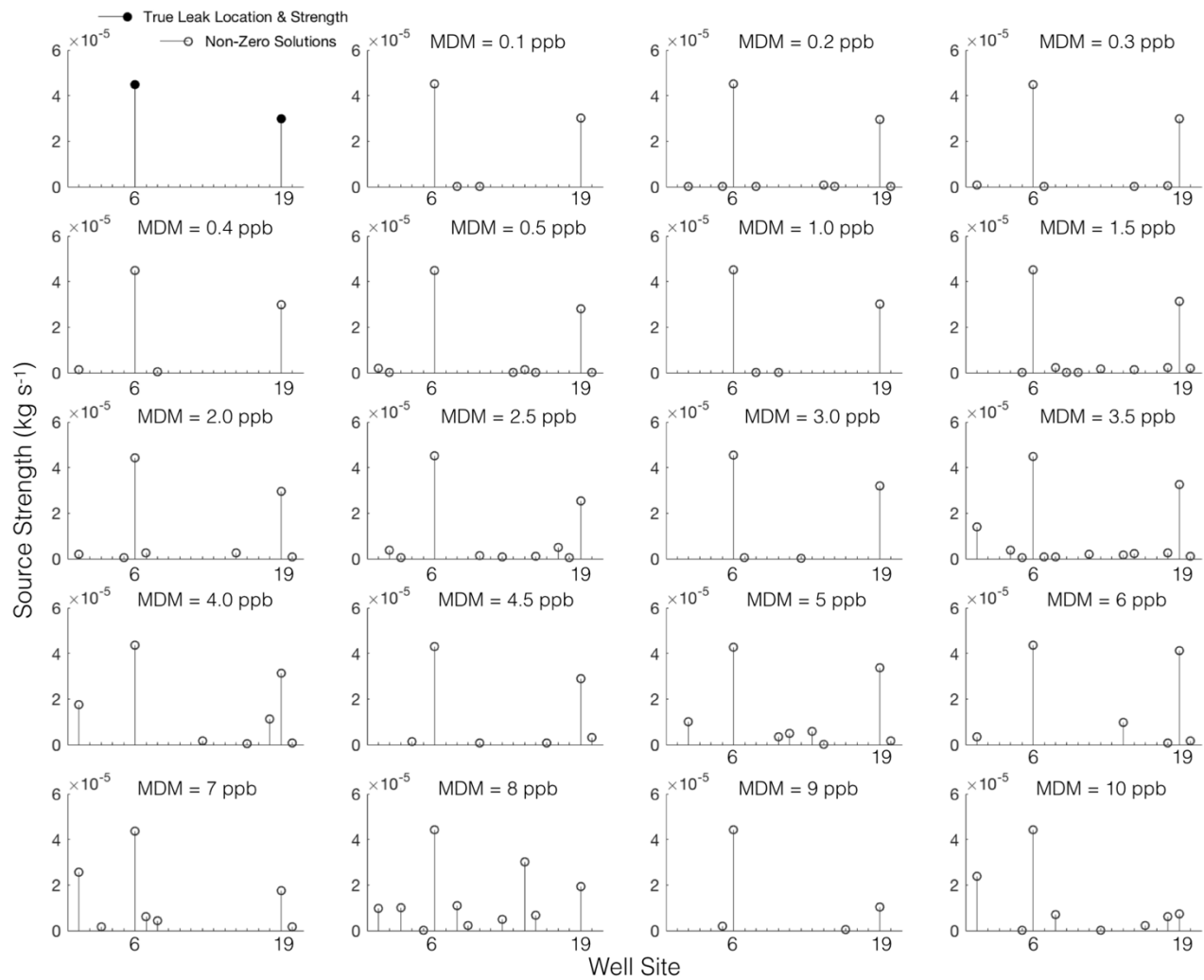
Figure S3: Same as Figure 12 in the main text, but calculated with an adjustment to the dispersion coefficient, σ_y . Histogram of NZMB estimated source strength at source location 2, with dashed line showing the bootstrap mean and thin dotted lines showing ± 2 standard deviation. The thick black line shows the true leak strength at source location 2 (0 kg s^{-1}). The presence of 0 kg s^{-1} in the histogram triggers acceptance of the null hypothesis (that the emissions rate at this site is zero).

5

10

Full range of Model-Data Mismatch Results

Here we show the full range of model-data mismatch results, which are not shown for the sake of avoiding figure complexity in Figures 5 and 6 in the main manuscript.



5 Figure S4: Same as main text Figure 5, but with all model-data mismatch cases shown.

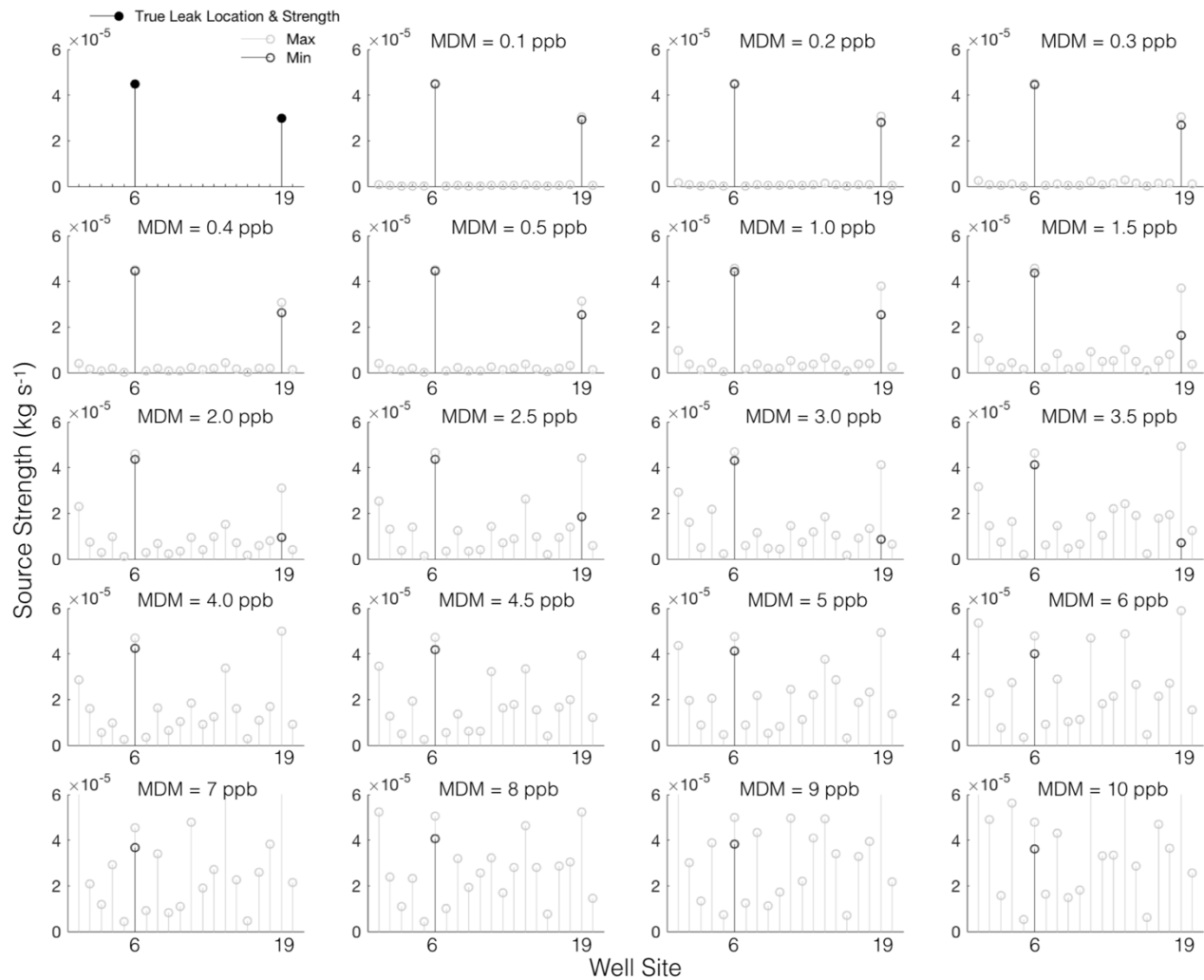


Figure S5: Same as main text Figure 6, but with all model-data mismatch cases shown.

Estimation of transport uncertainty

5 A simple estimate of transport uncertainty is derived by considering the combined impacts on simulated atmospheric concentrations of meteorological measurement instrument uncertainties, parameterization of atmospheric stability, and placement of the sonic anemometer relative to leak location (that is, the influence of using a point measurement of wind speed to characterize the entire wind field over the Table Mountain area). We use meteorological measurements made by two separate sonic anemometers placed at different locations (several hundred meters apart) on the Table Mountain site over the course of nearly 6 hours on March 3, 2017. Wind speed and wind direction are measured by both instruments. These meteorological measurements are used in a plume model simulation of the enhancement due to a leak with a rate equal to the controlled release of methane at source location 1 ($3.1E-5$ kg s $^{-1}$) along a 585 m beam that is either 9 m (the mean minimum lateral distance between each leak and adjacent beam in our test configuration) or 209 m (the mean distance between each leak and each segment of the beams directly monitoring it) downwind of the leak and perpendicular to wind direction. We calculate the standard deviation in the enhancement along the beam given the simulations with data from different

10

15

anemometers and given an increase and a decrease in the stability of one stability class from the mean state calculated on January 26th, 2017 (e.g., for a daily mean stability class of B, the absolute differences between B and A and B and C are averaged). This standard deviation is then taken to be the 1- σ uncertainty due to transport reported in the comparison to model-data mismatch in Section 4.4.

5 Note on units

The units ppb are equal to the SI units nmol mol⁻¹.

References

NOAA Earth System Research Laboratory: Surface Radiation Budget (SURFRAD) Network Observations. Radiation data from subset “Boulder_CO”. NOAA National Centers for Environmental Information. Accessed 2017.

- 10 Bailey, D. T.: Meteorological Monitoring Guidance for Regulatory Modeling Applications Meteorological Monitoring Guidance, Report No. EPA-454/R-99-005., 2000.

Briggs, G. A.: Diffusion estimation for small emissions, in ATDL Contribution File No. 79, Air Resources Atmospheric Turbulence and Diffusion Laboratory, NOAA, Oak Ridge, Tennessee., 1974.

Gifford, F. A.: Atmospheric dispersion models for environmental pollution, in Lectures on Air Pollution and Environmental Impact Analysis, edited by D. A. Haigen, pp. 35–58, Boston, Mass., 1976.

- 15 Griffiths, R. F.: Errors in the use of the Briggs parameterization for atmospheric dispersion coefficients, *Atmos. Environ.*, 28(17), 2861–2865, doi:doi:10.1016/1352-2310(94)90086-8, 1994.

Turner, D. B.: A diffusion model for an urban area, *J. Appl. Meteorol.*, 3, 83–91, 1964.